Published in final edited form as:
Arch Biochem Biophys. 2014 April 15; 548: 46–53. doi:10.1016/j.abb.2014.03.004.

Molecular and Functional Consequences of Mutations in the Central Helix of Cardiac Troponin C

Nicholas Swindle[‡], **Acchia N. J. Albury**[§], **Belal Baroud**[‡], **Maryam Burney**[‡], and **Svetlana B. Tikunova**[‡,*]

[‡]Department of Pharmacological and Pharmaceutical Sciences, University of Houston, Houston, TX 77004

[§]Department of Biology, Wingate University, Wingate, NC 28174

Abstract

The objective of this work was to investigate the role of acidic residues within the exposed middle segment of the central helix of cTnC in (1) cTnC-cTnI interactions, (2) Ca^{2+} binding and exchange with the regulatory N-domain of cTnC in increasingly complex biochemical systems, and (3) ability of the cTn complex to regulate actomyosin ATPase. In order to achieve this objective, we introduced the D87A/D88A and E94A/E95A/E96A mutations into the central helix of cTnC. The D87A/D88A and E94A/E95A/E96A mutations decreased affinity of cTnC for the regulatory region of cTnI. The Ca^{2+} sensitivity of the regulatory N-domain of isolated cTnC was decreased by the D87A/D88A, but not E94A/E95A/E96A mutation. However, both the D87A/D88A and E94A/E95A/E96A mutations desensitized the cTn complex and reconstituted thin filaments to Ca^{2+}. Decreases in the Ca^{2+} sensitivity of the cTn complex and reconstituted thin filaments were, at least in part, due to faster rates of Ca^{2+} dissociation. In addition, the D87A/D88A and E94A/E95A/E96A mutations desensitized actomyosin ATPase to Ca^{2+}, and decreased maximal actomyosin ATPase activity. Thus, our results indicate that conserved acidic residues within the exposed middle segment of the central helix of cTnC are important for the proper regulatory function of the cTn complex.

Keywords

Troponin C; Troponin I; Central helix; Fluorescence; Calcium binding

[*]To whom correspondence should be addressed: Svetlana B. Tikunova, Department of Pharmacological and Pharmaceutical Sciences, University of Houston, 521 Science and Research Building 2, Houston, TX 77204; Telephone: (713) 743-1224; Fax: (713) 743-1884; sbtikunova@uh.edu.

INTRODUCTION

Cardiac muscle utilizes troponin (cTn)[1] complex to regulate contraction-relaxation cycles in response to changes in intracellular Ca^{2+}. The hetero-trimeric cTn complex consists of cTnC (the Ca^{2+} binding subunit), cTnI (the inhibitory subunit), and cTnT (the tropomyosin (cTm)-binding subunit) (for review, see (1; 2)). At a resting level of intracellular Ca^{2+}, the cTn complex keeps cTm in a position that prevents force-producing interactions between myosin heads and actin. Increase in intracellular Ca^{2+} results in a series of conformational rearrangements in the cTn-cTm complex, allowing myosin heads to strongly bind actin (for review, see (3–9)).

The Ca^{2+} sensor cTnC consists of the N-and C-terminal globular domains connected by a flexible central α-helix. Each domain contains a pair of EF-hand (helix-loop-helix) Ca^{2+} binding motifs, numbered I–IV. The α-helices flanking the Ca^{2+} binding loops are denoted A–H. An additional 14-residue α-helix, denoted the N-helix, is located at the amino terminus. The nine-turn central helix connecting the two globular domains includes the D-helix of the N-domain, D/E helical linker and the E-helix of the C-domain (10; 11). The helical segments at the ends of the central helix are at least partially buried within the globular domains, while the middle three-turn segment is exposed to solvent (10; 11). The critical role of the central helix appears to be in properly orienting and positioning the two globular domains of cTnC for interactions with its targets (12).

Ca^{2+} binding and exchange with the N-domain of cTnC play a direct role in regulating cardiac muscle contractility, while the C-domain is believed to play a structural role of anchoring cTnC into the cTn complex (13; 14). The response of the regulatory N-domain of cTnC to Ca^{2+} is modulated by cTnI and other regulatory muscle proteins (15–17). CTnI contains an N-terminal extension region, an IT-arm region, the inhibitory region (which binds actin), the switch region and the C-terminal mobile domain (which contains second actin-binding site) (for review, see (18; 19)). The inhibitory region was determined to be important for both activation and inhibition of actomyosin ATPase (20). In the absence of Ca^{2+}, the inhibitory region binds to actin, preventing myosin heads from strongly binding actin. Binding of Ca^{2+} to the N-domain of cTnC allows the switch region of cTnI to bind to the hydrophobic patch on the N-domain of cTnC. This interaction leads to the removal of the inhibitory and C-domain actin-binding regions of cTnI from actin, resulting in shifting of the cTm position on the surface of actin and ultimately force generation (for review, see (6; 9)).

An overriding goal of our research is to elucidate the role of cTnC in the regulation of cardiac contractility. In this study, we have focused on the importance of acidic residues

[1]Abbreviations: TnC, troponin C; TnI, troponin I; cTnC, cardiac troponin C; $cTnC^{D87A/D88A}$, cTnC with the D87A/D88A mutation; $cTnC^{E94A/E95A/E96A}$, cTnC with the E94A/E95A/E96A mutation; cTnI, cardiac troponin I; $cTnI_{128\text{-}180}$, peptide corresponding to residues 128-180 of human cTnI; cTnT, cardiac troponin T; cTn, cardiac troponin complex: (cTnC-cTnI-cTnT); $cTn^{D87A/D88A}$, the cTn complex containing $cTnC^{D87A/D88A}$: ($cTnC^{D87A/D88A}$-cTnI-cTnT); $cTn^{E94A/E95A/E96A}$, the cTn complex containing $cTnC^{E94A/E95A/E96A}$: ($cTnC^{E94A/E95A/E96A}$-cTnI-cTnT); sTnC, skeletal troponin C; sTnI, skeletal troponin I; sTn, skeletal troponin complex; IAANS, 2-(4′-(iodoacetamido)anilino)naphthalene-6-sulfonic acid; EGTA, ethylene glycol-bis(2-aminoethyl)-N,N,N′,N′-tetraacetic acid; DTT, dithiothreitol; MOPS, 3-(N-morpholino)propanesulfonic acid; K_d, dissociation constant; k_{off}, dissociation rate.

located within the exposed middle segment of the central helix of cTnC. Functionally important residues tend to be conserved within a protein family (21; 22). The exposed middle segment of the central helix of cTnC contains negatively charged residues Asp^{87}, Asp^{88}, Glu^{94}, Glu^{95} and Glu^{96}. Sequence analysis indicates that these negatively charged residues are highly conserved among TnCs from different species and muscle types (23). In the crystal structure of the Ca^{2+} saturated skeletal Tn (sTn) complex, acidic residues within the exposed segment of the central helix of sTnC are involved in electrostatic interactions with basic residues within the inhibitory region of sTnI (24). On the other hand, the inhibitory region of cTnI was not visible in the crystal structure of the cTn complex (25). Thus, the importance of electrostatic interactions between the central helix of cTnC and the inhibitory region of cTnI is under debate.

The objective of our current study was to investigate the role of acidic residues within the exposed middle segment of the central helix in the interactions of cTnC with the regulatory region of cTnI (which includes both the inhibitory and switch regions, $cTnI_{128\text{-}180}$ (26; 27)). Furthermore, we wanted to determine whether these acidic residues influence Ca^{2+} binding and functional properties of cTnC. In order to achieve our objective, the Asp^{87}/Asp^{88} or Glu^{94}/Glu^{95}/Glu^{96} residues within the central helix of cTnC were mutated to neutral Ala residues. Ala was selected as a replacement residue in order to eliminate the side-chain interactions while maintaining the backbone conformation. Based on the assumption that in solution the cTn complex adopts a structure similar to the crystal structure of the sTn complex (28; 29), we expected our results to demonstrate the functional importance of acidic residues within the exposed middle segment of the central helix of cTnC.

EXPERIMENTAL PROCEDURES

Materials

Phenyl-Sepharose CL-4B, $CaCl_2$ and EGTA were purchased from Sigma-Aldrich (St. Louis, MO). IAANS and phalloidin were purchased from Invitrogen (Carlsbad, CA). Affi-Gel 15 affinity media were purchased from Bio-Rad (Hercules, CA). Malachite Green Oxalate and poly(vinyl alcohol) were purchased from Fisher Scientific (Pittsburgh, PA)

Protein Mutagenesis and Purification

The pET3a plasmid encoding human cTnC was a generous gift from Dr. Lawrence B. Smillie (University of Alberta, Edmonton, AB). The cTnC mutants were generated as previously described, and confirmed by DNA sequencing (15; 30). Expression and purification of cTnC and its mutants was carried out as previously described (15; 30; 31). The pET3d plasmids encoding human cTnI and human cTnT were generated by GenScript USA (Piscataway, NJ). The cTnI and cTnT subunits were bacterially expressed, purified and quantified as described (30). Rabbit fast skeletal actin and myosin S1, and bovine cTm were a general gift from Dr. Darl R. Swartz (Delaware Valley College (Doylestown, PA)).

Fluorescent Labeling of cTnC and its Mutants

cTnC proteins (with C35S/T53C/C84S substitution) were labeled with the environmentally sensitive thiol-reactive fluorescent probe IAANS on Cys^{53} as previously described (15; 30).

Determination of $cTnI_{128-180}$ Peptide Affinities

Fluorescence of IAANS attached to Cys^{53} of cTnC was monitored at 450 nm with excitation at 330 nm. Microliter amounts of $cTnI_{128-180}$ were added to 2 mL of each cTnC protein labeled with IAANS on Cys^{53} (0.15 μM) in buffer (10 mM MOPS, 150 mM KCl, 3 mM $MgCl_2$, 1 mM $CaCl_2$, 0.02 % Tween-20 and 1 mM DTT, at pH 7.0) at 15 °C with constant stirring. Each apparent peptide dissociation constant represents a means of at least three titrations ± SE fit to the root of quadratic equation for binary complex formation as previously described (30; 31).

Reconstitution of the cTn Complexes

The cTn complexes were prepared and reconstituted as previously described (15; 30).

Reconstitution of Thin Filaments

After exhaustive dialysis against reconstitution buffer (10 mM MOPS, 150 mM KCl, 3 mM $MgCl_2$, and 1 mM DTT, at pH 7.0), actin was mixed with an equal molar ratio of phalloidin to stabilize actin filaments. Thin filaments were reconstituted as previously described (15; 30). Briefly, actin-phalloidin (4 μM) and cTm (0.57μM) were mixed in the reconstitution buffer and kept on ice for ~ 15 minutes. The cTn complexes (0.5 μM) were subsequently added, and reconstituted thin filaments were kept on ice for at least 15 minutes prior to the experiments. To examine the effect of the central helix mutations on the Ca^{2+} binding properties of reconstituted thin filaments in the presence of myosin S1, myosin S1 (1.14 μM) was subsequently added, and thin filaments were kept on ice for at least 3 minutes prior to the experiments. Therefore, the stoichiometry of reconstituted thin filaments was 7:1:0.88:2 (actin:cTm:cTn:myosin S1).

Determination of Ca^{2+} Binding Sensitivities

All steady-state fluorescence measurements were performed using a Perkin-Elmer LS55 fluorescence spectrometer at 15 °C. Trp fluorescence was excited at 285 nm and monitored at 345 nm as μL amounts of $CaCl_2$ were added to 2 mL of each isolated cTnC protein (with F27W substitution (32)) in the titration buffer (200 mM MOPS (to prevent pH changes upon addition of Ca^{2+}), 150 mM KCl, 2 mM EGTA, 3 mM $MgCl_2$, and 1 mM DTT, at pH 7.0) with constant stirring. Fluorescence of IAANS attached to Cys^{53} of cTnC was excited at 330 nm and monitored at 450 nm or 490 nm as μL amounts of $CaCl_2$ were added to 2 mL of each cTn complex in the titration buffer (with 0.02 % Tween-20), or to reconstituted thin filaments with constant stirring. Thin filaments were reconstituted as described above, and diluted in half with an appropriate solution to achieve the same titration buffer composition. The $[Ca^{2+}]_{free}$ was calculated using the computer program EGCA02 developed by Robertson and Potter (33). The Ca^{2+} sensitivities of conformational changes were reported as a dissociation constant K_d, representing a mean of at least three titrations ± SE. The data were fit with a logistic sigmoid function (mathematically equivalent to the Hill equation), as previously described (34).

Determination of Ca^{2+} Dissociation Kinetics

All kinetic measurements were performed utilizing an Applied Photophysics Ltd. (Leatherhead, UK) model SX.18 MV stopped-flow instrument with a dead time of ~1.4 ms. The rates of conformational changes induced by EGTA (10 mM) removal of Ca^{2+} (500 μM) from the N-domain of isolated cTnC proteins (with F27W substitution) in the stopped-flow buffer (10 mM MOPS, 150 mM KCl, 3mM $MgCl_2$, and 1 mM DTT, at pH 7.0) were measured following Trp fluorescence at 15°C and 5°C. The Trp fluorescence was excited at 285 nm, with emission monitored through a WG320 filter from Newport Corporation (Irvine, CA). The rates of conformational changes induced by EGTA (10 mM) removal of Ca^{2+} (200 μM) from the cTn complexes in the stopped-flow buffer (with 0.02 % Tween-20), or from reconstituted thin filaments were measured at 15°C following fluorescence of IAANS attached to Cys^{53} of cTnC. Thin filaments were reconstituted as described above, and diluted in half with the stopped-flow buffer prior to the experiments. The IAANS fluorescence was excited at 330 nm, with emission monitored through a 510 nm BrightLine Basic™ filter from Semrock (Rochester, NY) or 515 nm cut-on filter from Newport Corporation (Irvine, CA). The data were corrected for scattering artifacts as described previously (15; 30). The data were fit using a program (by P. J. King, Applied Photophysics Ltd) that utilizes the nonlinear Levenberg-Marquardt algorithm. Each k_{off} represents an average of at least three separate experiments ± SE, each averaging at least five traces fit with a single exponential equation.

Actomyosin S1 ATPase Assay

Actomyosin ATPase assay was carried out as previously described (35). Briefly, reconstituted thin filaments (5μM actin, 1.0 μM cTm, 1.5 μM cTn, and 0.3 μM myosin S1) were formed at 25 °C in a buffer consisting of 50 mM MOPS, and 5 mM $MgCl_2$, pH 7.0. EGTA (to a final concentration of 0.5 mM) and various amounts of $CaCl_2$ were added to the 100 μL reaction mixture aliquots to achieve the desired pCa values. The ATPase reaction was initiated by addition of ATP (to a final concentration of 1 mM), and 10 μL aliquots were removed into 90 μL of 0.2M ice-cold perchloric acid in order to terminate the reaction. For determination of the Ca^{2+} dependence of actomyosin ATPase, the ATPase rates were measured at a single time point at which the reaction was still linear with time. In order to measure minimal and maximal specific actomyosin ATPase activities, 10 μL aliquots were terminated at 3 minute intervals (up to 12 minutes time course) by 90 μL of 0.2 M ice-cold perchloric acid. Actomyosin ATPase activity was determined by the amount of phosphate released. The amount of phosphate released was quantified using malachite green method, as previously described (30; 35).

Statistical Analysis

Statistical significance was determined by an unpaired two-sample t-test using the statistical analysis software Minitab (State College, PA). The two means were considered to be significantly different when the p value was < 0.05. All data is shown as a mean value ± SE.

RESULTS

Location of the Central Helix Residues within the Structure of cTnC Reconstituted into the cTn Complex

Figure 1 shows location of the Asp^{87}/Asp^{88} and Glu^{94}/Glu^{95}/Glu^{96} residues within the structure of cTnC reconstituted into the cTn complex (25). Figure 1 also shows that the central helix of cTnC was disordered, while the inhibitory region of cTnI was not visualized in the crystal structure of the cTn complex.

Effect of the Central Helix Mutations the on the Ca^{2+} Binding Properties of Isolated cTnC

Due to substitutions of several loop residues, the first EF-hand of cTnC is unable to bind Ca^{2+} under physiological conditions (36). The F27W substitution (32) was used to follow Ca^{2+} binding and exchange with the second EF-hand of isolated cTnC. Use of the F27W substitution was necessitated by the fact that in isolated cTnC, IAANS probe attached to Cys^{53} reflects conformational changes occurring within the structural C-domain sites (data not shown). Results of NMR spectroscopy suggested that the F27W substitution increases the Ca^{2+} sensitivity of the N-domain of cTnC (37). However, neither the D87A/D88A nor E94A/E95A/E96A mutation is located in close proximity to the F27W substitution. Thus, any possible effects of the F27W substitution are likely to be similar between cTnC and central helix mutants, allowing us to accurately quantify differences in the Ca^{2+} sensitivity of the N-domain.

The Ca^{2+}-induced increases in Trp fluorescence, which occur when Ca^{2+} binds to the regulatory N-domain of cTnC or its mutants, are shown in Figure 2A. Results are summarized in Table I. The cTnC exhibited a half-maximal Ca^{2+}-dependent increase in Trp fluorescence at 28 ± 2 μM. The D87A/D88A mutation led to ~1.6-fold decrease in the Ca^{2+} sensitivity of cTnC, while the E94A/E95A/E96A mutation did not significantly affect the Ca^{2+} sensitivity of cTnC (Figure 2A and Table I). The Hill coefficients (as indicated by the n_H values) for the Ca^{2+} titrations were between 0.88 and 1.03, consistent with binding of single Ca^{2+} ion to the second EF-hand of cTnC (Table I).

Stopped-flow measurements, utilizing Trp fluorescence, were conducted to examine the effect of the central helix mutations on the rate of Ca^{2+} dissociation from the N-domain of isolated cTnC. Results are summarized in Table I. At 15°C, excess EGTA removed Ca^{2+} from the regulatory N-domain of cTnC at 1349 ± 56 s^{-1}. At 15°C, the D87A/D88A and E94A/E95A/E96A mutations did not significantly affect rates of Ca^{2+} dissociation from the N-domain of isolated cTnC (Figure 2B and Table I). Since these k_{off} values are close to the upper limit of rates that can be measured in the stopped-flow apparatus, rates of Ca^{2+} dissociation from the N-domain of isolated cTnC were also measured at 5°C. At 5°C, excess EGTA removed Ca^{2+} from the regulatory N-domain of cTnC, $cTnC^{D87A/D88A}$, or $cTnC^{E94A/E95A/E96A}$ at 915 ± 9, 896 ± 8, or 886 ± 21 s^{-1}, respectively (Figure 2C). Thus, our results demonstrate that the central helix mutations had very little effect on the rates of Ca^{2+} dissociation at either 15°C or 5°C.

Effect of the Central Helix Mutations on the Affinity of cTnC for the Regulatory Region of cTnI

The effect of the central helix mutations on the affinity of cTnC for the $cTnI_{128-180}$ was measured following changes in fluorescence of IAANS attached to Cys^{53} of cTnC (30). Figure 3 shows that $cTnI_{128-180}$ peptide binds to the Ca^{2+}-saturated cTnC with a dissociation constant of 62 ± 5 nM. Figure 3 also shows that $cTnI_{128-180}$ peptide binds to the Ca^{2+}-saturated $cTnC^{D87A/D88A}$ or $cTnC^{E94A/E95A/E96A}$ with a dissociation constant of 174 ± 22 or 156 ± 6 nM, respectively. Thus, the D87A/D88A and E94A/E95A/E96A mutations significantly decreased the affinity of cTnC for $cTnI_{128-180}$ by ~2.8- and 2.5-fold, respectively.

Effect of the Central Helix Mutations on the Ca^{2+} Binding Properties of the cTn Complex

The Ca^{2+}-induced decreases in IAANS fluorescence, which occur when Ca^{2+} binds to the regulatory N-domain of cTnC or its mutants reconstituted into the cTn complexes, are shown in Figure 4A. Results are summarized in Table I. The cTn complex exhibited a half-maximal Ca^{2+}-dependent decrease in IAANS fluorescence at 0.83 ± 0.07 μM. The D87A/D88A and E94A/E95A/E96A mutations led to ~3.0- and 2.2-fold decreases, respectively, in the Ca^{2+} sensitivity of the cTn complex. Neither the D87A/D88A nor E94A/E95A/E96A mutation affected the cooperativity of Ca^{2+} binding to the cTn complex (as indicated by the n_H values) (Table I).

Stopped-flow measurements, utilizing IAANS fluorescence, were conducted to examine the effect of the central helix mutations on the rate of Ca^{2+} dissociation from the cTn complex. Results are summarized in Table I. Figure 4B shows that excess EGTA removed Ca^{2+} from the regulatory N-domain of cTnC reconstituted into the cTn complex at 42.3 ± 0.2 s^{-1}. The D87A/D88A and E94A/E95A/E96A mutations led to ~1.9- and 1.5-fold faster, respectively, rates of Ca^{2+} dissociation from the cTn complex (Figure 4B and Table I).

Effect of the Central Helix Mutations on the Ca^{2+} Binding Properties of Reconstituted Thin Filaments

The Ca^{2+}-induced changes in IAANS fluorescence, which occur when Ca^{2+} binds to the regulatory N-domain of the cTn, $cTn^{D87A/D88A}$, or $cTn^{E94A/E95A/E96A}$ complexes reconstituted into thin filaments, are shown in Figure 5A. Results are summarized in Table I. After reconstitution into thin filaments, the cTn complex exhibited a half-maximal Ca^{2+}-dependent increase in IAANS fluorescence at 2.15 ± 0.09 μM. The D87A/D88A and E94A/E95A/E96A mutations led to ~4.7- and 5.6- fold decreases, respectively, in the Ca^{2+} sensitivities of the cTn complex reconstituted into thin filaments (Figure 5A and Table I). Furthermore, the D87A/D88A mutation decreased the cooperativity of Ca^{2+} binding to reconstituted thin filaments (indicated by a lower n_H), suggesting that this mutation affected near-neighbor regulatory unit interactions along the thin filament. The E94A/E95A/E96A mutation had no effect on cooperativity (Table I).

Stopped-flow measurements, utilizing IAANS fluorescence, were conducted to determine the effect of the central helix mutations on the kinetics of Ca^{2+} dissociation from the regulatory N-domain of the cTn complex reconstituted into thin filaments. The results are

summarized in Table I. Figure 5B shows that excess EGTA removed Ca^{2+} from the cTn complex reconstituted into thin filaments at 93 ± 1 s^{-1}. The D87A/D88A and E94A/E95A/E96A mutations led to ~1.8-fold acceleration in the rate of Ca^{2+} dissociation from the cTn complex reconstituted into thin filaments (Figure 5B and Table I).

Effect of the Central Helix Mutations on the Ca^{2+} Binding Properties of Reconstituted Thin Filaments in the Presence of Myosin S1

The Ca^{2+}-induced increases in IAANS fluorescence, occurring when Ca^{2+} binds to the regulatory N-domain of the cTn, $cTn^{D87A/D88A}$, or $cTn^{E94A/E95A/E96A}$ complexes, reconstituted into thin filaments in the presence of myosin S1, are shown in Figure 6A and summarized in Table I. In the presence of two myosin S1 molecules per stoichiometric unit, the cTn complex reconstituted into thin filaments exhibited a half-maximal Ca^{2+} dependent increase in IAANS fluorescence at 0.29 ± 0.02 μM. Our results show that in the presence of myosin S1, the D87A/D88A mutation led to ~6.0-fold decrease in the Ca^{2+} sensitivity of reconstituted thin filaments, while the E94A/E95A/E96A mutation led to ~12.8-fold decrease in the Ca^{2+} sensitivity of reconstituted thin filaments (Figure 6A and Table I). Furthermore, our results show that neither the D87A/D88A nor E94A/E95A/E96A mutation significantly affected the cooperativity of Ca^{2+} binding to reconstituted thin filaments in the presence of myosin S1 (Table I).

Stopped-flow measurements, utilizing IAANS fluorescence, were conducted to determine the effect of the central helix mutations on the kinetics of Ca^{2+} dissociation from the regulatory N-domain of the cTn complex reconstituted into thin filaments in the presence of myosin S1. The results are summarized in Table I. Figure 6B shows that excess EGTA removed Ca^{2+} from the cTn complex reconstituted into thin filaments in the presence of myosin S1 at 11.7 ± 0.2 s^{-1}. Our results show that both the D87A/D88A and E94A/E95A/E96A mutations led to ~1.8-fold faster rate of Ca^{2+} dissociation from the cTn complex reconstituted into thin filaments in the presence of myosin S1 (Figure 6B and Table I).

Effect of the Central Helix Mutations on the Specific Activities and Ca^{2+} Sensitivities of Actomyosin ATPase

First, we evaluated the effect of the central helix mutations on the specific activities of actomyosin ATPase at pCa 9.0 and 4.5. The results are summarized in Table II and are shown in Figure 7A. Our results demonstrate that the central helix mutations enhanced the ability of the cTn complex to inhibit actomyosin ATPase in the absence of Ca^{2+}. Our results also show that in the presence of saturating Ca^{2+}, the central helix mutations substantially impaired the ability of the cTn complex to activate actomyosin ATPase.

Next, we examined the effect of the central helix mutations on the Ca^{2+} sensitivity of actomyosin ATPase. For thin filaments reconstituted with the cTn complex, half-maximal Ca^{2+} activation occurred at 1.49 ± 0.03 μM (Figure 7B and Table II). Our results indicate that both the D87A/D88A and E94A/E95A/E96A mutations led to a ~1.9-fold decrease in the Ca^{2+} sensitivity of actomyosin ATPase (Figure 7B and Table II). The n_H values for actomyosin ATPase curves were not significantly affected by either the D87A/D88A or E94A/E95A/E96A mutation (Table II).

DISCUSSION

In this study, we investigated the molecular and functional consequences of the D87A/D88A and E94A/E95A/E96A mutations. We determined that the D87A/D88A but not E94A/E95A/E96A mutation resulted in the lower Ca^{2+} sensitivity of the N-domain of isolated cTnC. However, both the D87A/D88A and E94A/E95A/E96A mutations resulted in the substantially lower affinity of Ca^{2+} saturated cTnC for the regulatory region of cTnI ($cTnI_{128-180}$), potentially due to the loss of electrostatic interactions between acidic residues within the central helix of cTnC and basic residues within the inhibitory region of cTnI.

In muscle, cTnC does not function in isolation but as a part of the cTn complex. Binding of cTnI substantially increases the Ca^{2+} sensitivity of cTnC (17), by stabilizing the “open” state of the regulatory N-domain (38; 39). Our results indicate that desensitization of the cTn complex to Ca^{2+} by the D87A/D88A and E94A/E95A/E96A mutations was largely due to the faster rates of Ca^{2+} dissociation. The D87A/D88A and E94A/E95A/E96A mutations had an even larger impact on the Ca^{2+} desensitization of the cTn complex after reconstitution into thin filaments (in the absence or presence of myosin S1). Decreased affinity of cTnC for the regulatory region of cTnI could lead to the increased probability of interactions between the inhibitory region of cTnI and actin, thus enhancing ability of the central helix mutations to desensitize thin filaments to Ca^{2+}. The Ca^{2+} desensitization was not solely due to the faster rates of Ca^{2+} dissociation, indicating that the central helix mutations decreased the rates of Ca^{2+} association to the cTn complex reconstituted into thin filaments (in the absence or presence of myosin S1). Thus, central helix mutations appear to stabilize the “closed” state of the regulatory N-domain of cTnC within the cTn complex reconstituted into thin filaments (in the absence or presence of myosin S1), in addition to destabilizing the “open” state. Our findings are consistent with those from earlier studies, which showed that naturally occurring and engineered cTnC mutations can alter the rates of Ca^{2+} association to the cTn complex reconstituted into increasingly complex biochemical systems (40).

TnC exists in two isoforms, one found in cardiac and slow skeletal muscle (cTnC), the other found in fast skeletal muscle (sTnC). A number of earlier studies focused on elucidating the role of central helix in the biophysical properties and biological function of sTnC (41–48). Flexibility and length of the central helix were shown to play a role in the proper regulatory function of sTnC (42; 48). Much less is known about the significance of central helix to the function of cTnC. For instance, an earlier study determined that the D88A mutation did not affect the Ca^{2+} sensitivity of isolated cTnC (49). However, that study (49) did not examine the effect of the D88A mutation on the Ca^{2+} binding properties of cTnC reconstituted into more complex biochemical systems. Crystal structures of Ca^{2+} bound cTn (25) and sTn (24) complexes show similar overall organization of the subunits. However, there are a number of differences, including the orientation of the regulatory N-domain and conformation of the central helix of TnC, and the structure of the inhibitory region of TnI. In the crystal structure of the sTn complex, well ordered inhibitory region of sTnI was shown to interact with the rigid central helix of sTnC. On the other hand, in the crystal structure of the cTn complex, the central helix of cTnC was disordered, and the inhibitory region of cTnI was not visualized. Hydrogen-deuterium exchange mass spectroscopy and ^{15}N NMR relaxation studies suggest that in solution the cTn complex adopts a structure more similar to that of

the crystal structure of the sTn complex (28; 29). Our results are consistent with the idea that, in the presence of Ca^{2+}, acidic residues within the exposed segment of the central helix of cTnC come in close contact with basic residues in the inhibitory region of cTnI, such as Lys^{139}, Arg^{140}, Arg^{144} and Arg^{145}.

Both the D87A/D88A and E94A/E95A/E96A mutations desensitized actomyosin ATPase to Ca^{2+} and decreased maximal ATPase activity. Regarding the functional significance of the Asp^{87}/Asp^{88} cluster, our results are in agreement with those observed for sTnC, where the D89A mutation in chicken sTnC (which corresponds to the D88A mutation in cTnC) led to diminished ability of the sTn complex to activate actomyosin ATPase in the presence of saturating Ca^{2+} (41). Similarly, the E88K mutation in chicken sTnC was shown to decrease the Ca^{2+} sensitivity of force development and reduce tension recovery in skinned muscle fibers (44). In this work, we show for the first time that the $Glu^{94}/Glu^{95}/Glu^{96}$ cluster is as important to the proper regulatory function of the cTn complex as the Asp^{87}/Asp^{88} cluster.

It is important to note that we used skeletal actin and myosin S1 in this study because of our extensive prior work using these proteins (15; 30; 35; 40; 50). However, skeletal and cardiac actins are 99 % identical, differing by only four amino acids. In addition, results of a recent study (51) examining effects of human recombinant cardiac myosin S1 (with both rigor and cycling myosin S1) on the Ca^{2+} sensitivity of thin filaments agreed with the results from our earlier study which used skeletal myosin S1(15). Thus, it is highly unlikely that use of skeletal actin and myosin S1 had a major effect on the outcomes of our current study.

It is well accepted that altered Ca^{2+} binding and exchange with thin filaments can lead to adverse physiological consequences. Mutations of sarcomeric proteins associated with dilated cardiomyopathy (DCM) tend to reduce Ca^{2+} sensitivity of actomyosin ATPase and lower maximal ATPase activity (52–55). Functional consequences of the D87A/D88A and E94A/E95A/E96A mutations are consistent with those of known mutations associated with the DCM phenotype. In vivo studies are needed to determine whether central helix mutations examined in this work can recapitulate the pathogenesis of DCM.

In conclusion, our results demonstrate the importance of acidic residues within the exposed middle segment of the central helix of cTnC in controlling: 1) affinity of cTnC for the regulatory fragment of cTnI, 2) Ca^{2+} binding and exchange with the cTn complex in increasingly complex biochemical systems, and 3) ability of the cTn complex to regulate actomyosin ATPase.

Acknowledgments

We thank Dr. Lawrence Smillie (University of Alberta) for the generous gift of the human cTnC plasmid. We also thank Dr. Darl Swartz (Delaware Valley College) for the generous gift of actin, cTm and myosin S1. Research reported in this publication was supported by the NHLBI institute of NIH under Award Number R15HL117034 (to S.B.T). The content is solely the responsibility of the authors, and does not necessarily represent the official views of the NIH.

References

1. Filatov VL, Katrukha AG, Bulargina TV, Gusev NB. Biochemistry (Mosc). 1999; 64:969–985. [PubMed: 10521712]

2. Farah CS, Reinach FC. Faseb J. 1995; 9:755–767. [PubMed: 7601340]
3. Davis JP, Tikunova SB. Cardiovasc Res. 2008; 77:619–626. [PubMed: 18079104]
4. Kobayashi T, Jin L, de Tombe PP. Pflugers Arch. 2008; 457:37–46. [PubMed: 18421471]
5. Kobayashi T, Solaro RJ. Annu Rev Physiol. 2005; 67:39–67. [PubMed: 15709952]
6. Gordon AM, Homsher E, Regnier M. Physiol Rev. 2000; 80:853–924. [PubMed: 10747208]
7. Li MX, Wang X, Sykes BD. J Muscle Res Cell Motil. 2004; 25:559–579. [PubMed: 15711886]
8. Tobacman LS. Annu Rev Physiol. 1996; 58:447–481. [PubMed: 8815803]
9. Gordon AM, Regnier M, Homsher E. News Physiol Sci. 2001; 16:49–55. [PubMed: 11390948]
10. Sundaralingam M, Bergstrom R, Strasburg G, Rao ST, Roychowdhury P, Greaser M, Wang BC. Science. 1985; 227:945–948. [PubMed: 3969570]
11. Herzberg O, James MN. Nature. 1985; 313:653–659. [PubMed: 3974698]
12. Matsumoto F, Makino K, Maeda K, Patzelt H, Maeda Y, Fujiwara S. J Mol Biol. 2004; 342:1209–1221. [PubMed: 15351646]
13. Reinach FC, Farah CS, Monteiro PB, Malnic B. Cell Struct Funct. 1997; 22:219–223. [PubMed: 9113410]
14. Potter JD, Gergely J. J Biol Chem. 1975; 250:4628–4633. [PubMed: 124731]
15. Davis JP, Norman C, Kobayashi T, Solaro RJ, Swartz DR, Tikunova SB. Biophys J. 2007; 92:3195–3206. [PubMed: 17293397]
16. Kobayashi T, Solaro RJ. J Biol Chem. 2006; 281:13471–13477. [PubMed: 16531415]
17. Johnson JD, Collins JH, Robertson SP, Potter JD. J Biol Chem. 1980; 255:9635–9640. [PubMed: 7430090]
18. Solaro RJ, Rosevear P, Kobayashi T. Biochem Biophys Res Commun. 2008; 369:82–87. [PubMed: 18162178]
19. Tardiff JC. Circ Res. 2011; 108:765–782. [PubMed: 21415410]
20. Kobayashi T, Patrick SE, Kobayashi M. J Biol Chem. 2009; 284:20052–20060. [PubMed: 19483081]
21. Guharoy M, Chakrabarti P. BMC Bioinformatics. 2010; 11:286. [PubMed: 20507585]
22. Godzik A, Sander C. Protein Eng. 1989; 2:589–596. [PubMed: 2813336]
23. Collins JH. J Muscle Res Cell Motil. 1991; 12:3–25. [PubMed: 2050809]
24. Vinogradova MV, Stone DB, Malanina GG, Karatzaferi C, Cooke R, Mendelson RA, Fletterick RJ. Proc Natl Acad Sci U S A. 2005; 102:5038–5043. [PubMed: 15784741]
25. Takeda S, Yamashita A, Maeda K, Maeda Y. Nature. 2003; 424:35–41. [PubMed: 12840750]
26. Sorsa T, Pollesello P, Permi P, Drakenberg T, Kilpelainen I. J Mol Cell Cardiol. 2003; 35:1055–1061. [PubMed: 12967628]
27. Sorsa T, Pollesello P, Rosevear PR, Drakenberg T, Kilpelainen I. Eur J Pharmacol. 2004; 486:1–8. [PubMed: 14751401]
28. Lindhout DA, Boyko RF, Corson DC, Li MX, Sykes BD. Biochemistry. 2005; 44:14750–14759. [PubMed: 16274223]
29. Kowlessur D, Tobacman LS. J Biol Chem. 2010; 285:2686–2694. [PubMed: 19920153]
30. Tikunova SB, Liu B, Swindle N, Little SC, Gomes AV, Swartz DR, Davis JP. Biochemistry. 2010; 49:1975–1984. [PubMed: 20128626]
31. Swindle N, Tikunova SB. Biochemistry. 2010; 49:4813–4820. [PubMed: 20459070]
32. Tikunova SB, Davis JP. J Biol Chem. 2004; 279:35341–35352. [PubMed: 15205455]
33. Robertson S, Potter JD. Methods in Pharmacology. 1984; 5:63–75.
34. Tikunova SB, Rall JA, Davis JP. Biochemistry. 2002; 41:6697–6705. [PubMed: 12022873]
35. Albury AN, Swindle N, Swartz DR, Tikunova SB. Biochemistry. 2012; 51:3614–3621. [PubMed: 22489623]
36. van Eerd JP, Takahashi K. Biochem Biophys Res Commun. 1975; 64:122–127. [PubMed: 1170846]
37. Gillis TE, Blumenschein TM, Sykes BD, Tibbits GF. Biochemistry. 2003; 42:6418–6426. [PubMed: 12767223]

38. Li MX, Spyracopoulos L, Sykes BD. Biochemistry. 1999; 38:8289–8298. [PubMed: 10387074]
39. Dong WJ, Xing J, Villain M, Hellinger M, Robinson JM, Chandra M, Solaro RJ, Umeda PK, Cheung HC. J Biol Chem. 1999; 274:31382–31390. [PubMed: 10531339]
40. Liu B, Tikunova SB, Kline KP, Siddiqui JK, Davis JP. PLoS One. 2012; 7:e38259. [PubMed: 22675533]
41. Ramakrishnan S, Hitchcock-DeGregori SE. Biochemistry. 1996; 35:15515–15521. [PubMed: 8952505]
42. Babu A, Rao VG, Su H, Gulati J. J Biol Chem. 1993; 268:19232–19238. [PubMed: 8366076]
43. Dobrowolski Z, Xu GQ, Hitchcock-DeGregori SE. J Biol Chem. 1991; 266:5703–5710. [PubMed: 1826002]
44. Fujimori K, Sorenson M, Herzberg O, Moult J, Reinach FC. Nature. 1990; 345:182–184. [PubMed: 2186281]
45. Ding XL, Akella AB, Su H, Gulati J. Protein Sci. 1994; 3:2089–2096. [PubMed: 7703855]
46. Sundaralingam M, Drendel W, Greaser M. Proc Natl Acad Sci U S A. 1985; 82:7944–7947. [PubMed: 3865207]
47. Kobayashi T, Zhao X, Wade R, Collins JH. Biochim Biophys Acta. 1999; 1430:214–221. [PubMed: 10082949]
48. Ramakrishnan S, Hitchcock-DeGregori SE. Biochemistry. 1995; 34:16789–16796. [PubMed: 8527454]
49. Pollesello P, Ovaska M, Kaivola J, Tilgmann C, Lundstrom K, Kalkkinen N, Ulmanen I, Nissinen E, Taskinen J. J Biol Chem. 1994; 269:28584–28590. [PubMed: 7961805]
50. Liu B, Lee RS, Biesiadecki BJ, Tikunova SB, Davis JP. J Biol Chem. 2012; 287:20027–20036. [PubMed: 22511780]
51. Sommese RF, Nag S, Sutton S, Miller SM, Spudich JA, Ruppel KM. PLoS One. 2013; 8:e83403. [PubMed: 24367593]
52. Morimoto S, Lu QW, Harada K, Takahashi-Yanaga F, Minakami R, Ohta M, Sasaguri T, Ohtsuki I. Proc Natl Acad Sci U S A. 2002; 99:913–918. [PubMed: 11773635]
53. Pinto JR, Siegfried JD, Parvatiyar MS, Li D, Norton N, Jones MA, Liang J, Potter JD, Hershberger RE. J Biol Chem. 2011; 286:34404–34412. [PubMed: 21832052]
54. Mirza M, Marston S, Willott R, Ashley C, Mogensen J, McKenna W, Robinson P, Redwood C, Watkins H. J Biol Chem. 2005; 280:28498–28506. [PubMed: 15923195]
55. Robinson P, Griffiths PJ, Watkins H, Redwood CS. Circ Res. 2007; 101:1266–1273. [PubMed: 17932326]
56. Guex N, Peitsch MC. Electrophoresis. 1997; 18:2714–2723. [PubMed: 9504803]

D87A/D88A and E94A/E95A/E96A mutations were introduced into the central helix of cTnC

Central helix mutations decreased affinity of Ca^{2+} saturated cTnC for $cTnI_{128-180}$

Central helix mutations desensitized the cTn complex and thin filaments to Ca^{2+}

Central helix mutations decreased the Ca^{2+} sensitivity of actomyosin ATPase

Central helix mutations decreased maximal activity of actomyosin ATPase

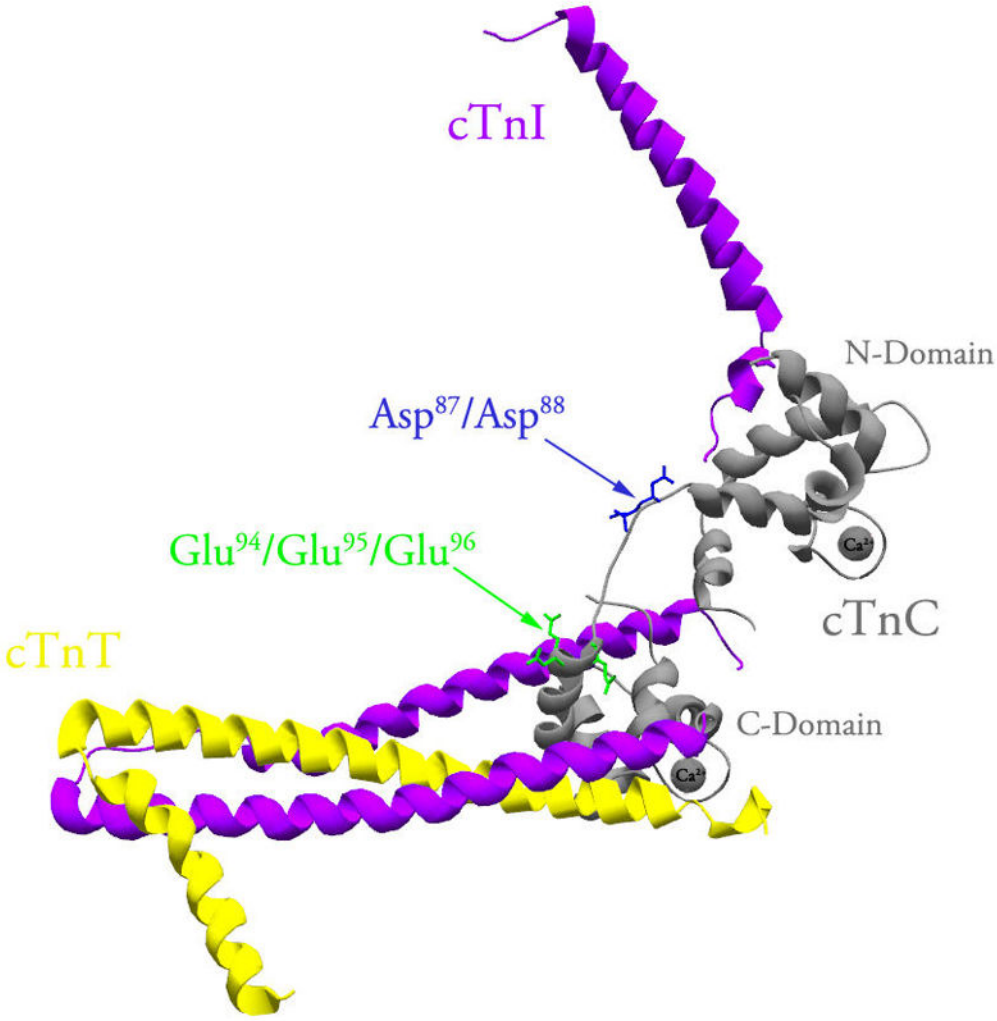

Figure 1. Location of the central helix residues within the structure of cTnC reconstituted into the cTn complex

The figure shows a ribbon representation of the core domain of the cTn complex in the Ca^{2+} bound state (Protein Data Bank entry 1J1E (25)). CTnC, cTnI and cTnT are colored in grey, magenta and yellow, respectively. The Asp^{87}/Asp^{88} residues (shown in blue) and $Glu^{94}/Glu^{95}/Glu^{96}$ residues (shown in green) are located within the exposed middle segment of the central helix of cTnC. This figure was generated using Swiss-PdbViewer (56).

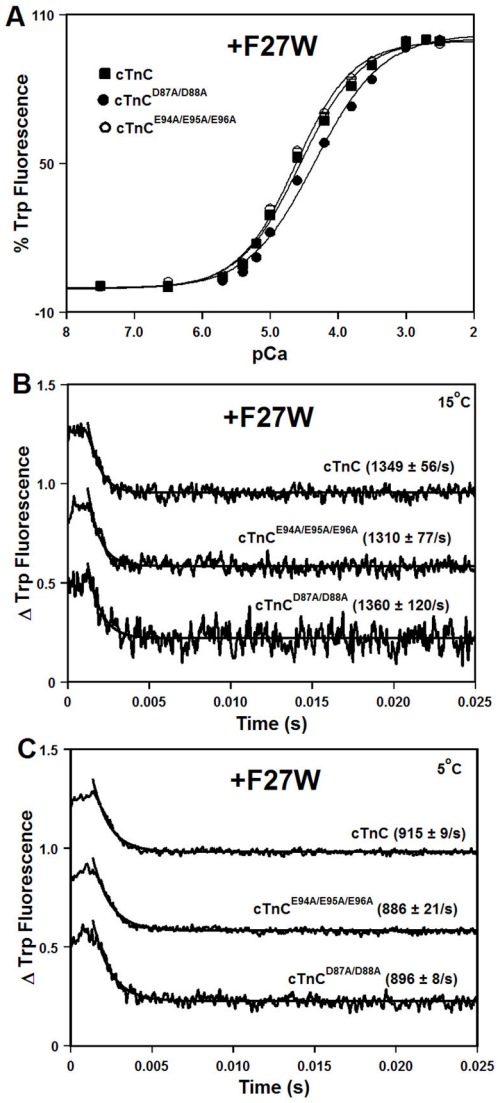

Figure 2. Effect of the central helix mutations on the Ca^{2+} binding properties of isolated cTnC

Panel A shows increases in Trp fluorescence, which occur as Ca^{2+} binds to the N-domains of cTnC (■), $cTnC^{D87A/D88A}$ (●), or $cTnC^{E94A/E95A/E96A}$ (○) at 15°C. The cTnC proteins contained F27W substitution. The Trp fluorescence was excited at 285 nm and monitored at 345 nm. Panels B and C show the time course of decreases in Trp fluorescence as Ca^{2+} was removed by excess EGTA from the N-domains of isolated cTnC, $cTnC^{D87A/D88A}$, or $cTnC^{E94A/E95A/E96A}$. Panel B: measured at 15°C. Panel C: measured at 5°C. The data traces have been normalized and staggered for clarity. Each trace is an average of at least five traces fit with a single exponential equation. The Trp fluorescence was excited at 285 nm and monitored through a WG320 filter.

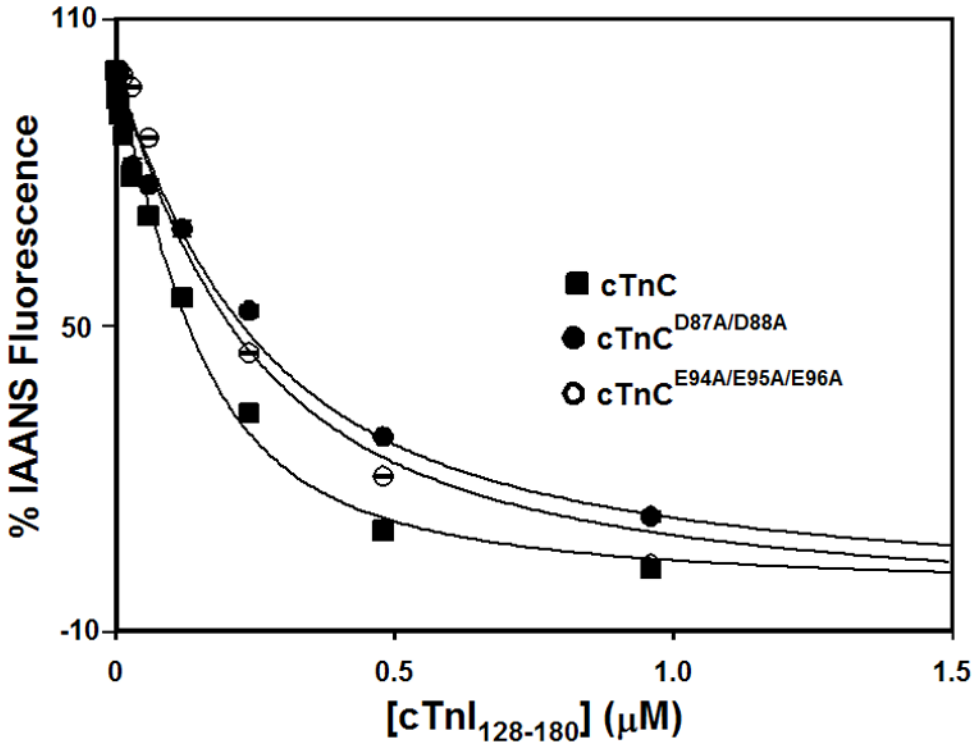

Figure 3. Effect of the central helix mutations on the affinity of cTnC for the regulatory region of cTnI

Figure shows the effect of central helix mutations on the $cTnI_{128-180}$ binding properties of cTnC in the presence of 1 mM Ca^{2+} at 15°C. The $cTnI_{128-180}$-dependent decreases in IAANS fluorescence are shown as a function of [$cTnI_{128-180}$] for cTnC (■), $cTnC^{D87A/D88A}$ (●), or $cTnC^{E94A/E95A/E96A}$ (○). The cTnC proteins (with C35S/T53C/C84S substitution) were labeled with IAANS at Cys^{53}. 100 % IAANS fluorescence corresponds to the Ca^{2+}-bound state, whereas 0% fluorescence corresponds to the Ca^{2+}-$cTnI_{128-180}$ bound state for each individual cTnC protein.

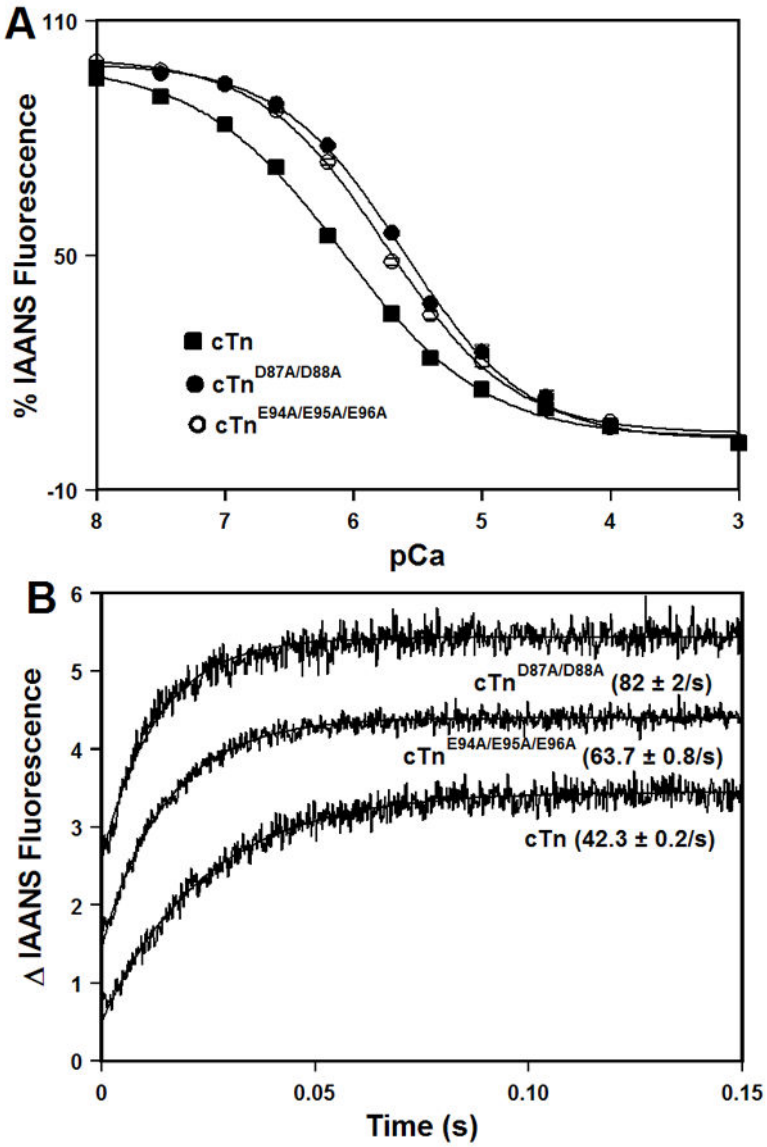

Figure 4. Effect of the central helix mutations on the Ca^{2+} binding properties of the cTn complex

Panel A shows decreases in IAANS fluorescence, which occur as Ca^{2+} binds to the cTn (■), $cTn^{D87A/D88A}$ (●), or $cTn^{E94A/E95A/E96A}$ (○) complexes at 15°C. The cTnC proteins (with C35S/T53C/C84S substitution) were labeled with IAANS at Cys^{53}. The IAANS fluorescence was excited at 330 nm and monitored at 450 nm. Panel B shows the time course of increases in IAANS fluorescence as Ca^{2+} was removed by excess EGTA from the cTn, $cTn^{D87A/D88A}$, or $cTn^{E94A/E95A/E96A}$ complexes at 15°C. The data traces have been normalized and staggered for clarity. Each trace is an average of at least five traces fit with a single exponential equation. The IAANS fluorescence was excited at 330 nm and monitored through a 510 nm band-pass filter.

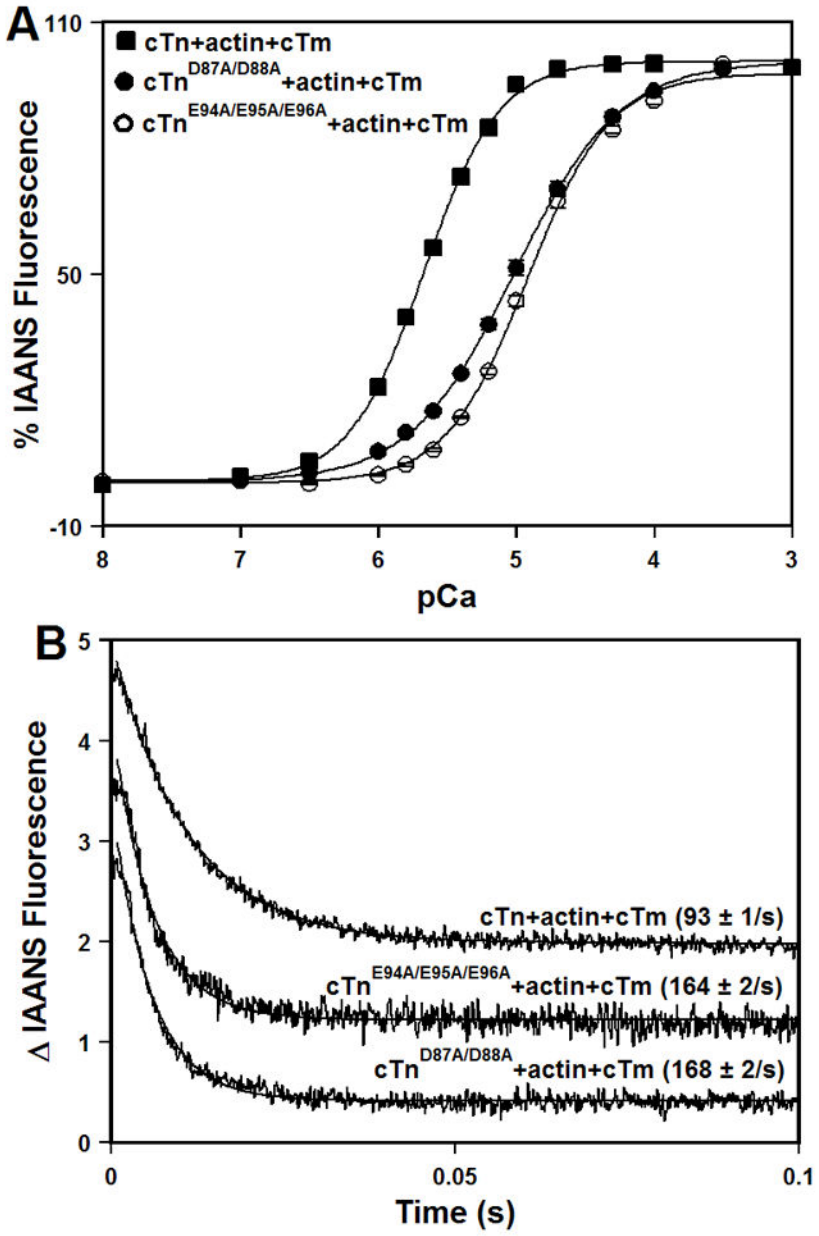

Figure 5. Effect of the central helix mutations on the Ca^{2+} binding properties of reconstituted thin filaments

Panel A shows increases in IAANS fluorescence, which occur as Ca^{2+} binds to the cTn (■), $cTn^{D87A/D88A}$ (●), or $cTn^{E94A/E95A/E96A}$ (○) complexes reconstituted into thin filaments at 15°C. The cTnC proteins (with C35S/T53C/C84S substitution) were labeled with IAANS at Cys^{53}. The IAANS fluorescence was excited at 330 nm and monitored at 450 nm. Panel B shows the time course of decreases in IAANS fluorescence as Ca^{2+} was removed by excess EGTA from the cTn, $cTn^{D87A/D88A}$, or $cTn^{E94A/E95A/E96A}$ complexes reconstituted into thin filaments at 15°C. The data traces have been normalized and staggered for clarity. Each trace is an average of at least five traces fit with a single exponential equation. The IAANS fluorescence was excited at 330 nm and monitored through a 510 nm band-pass filter.

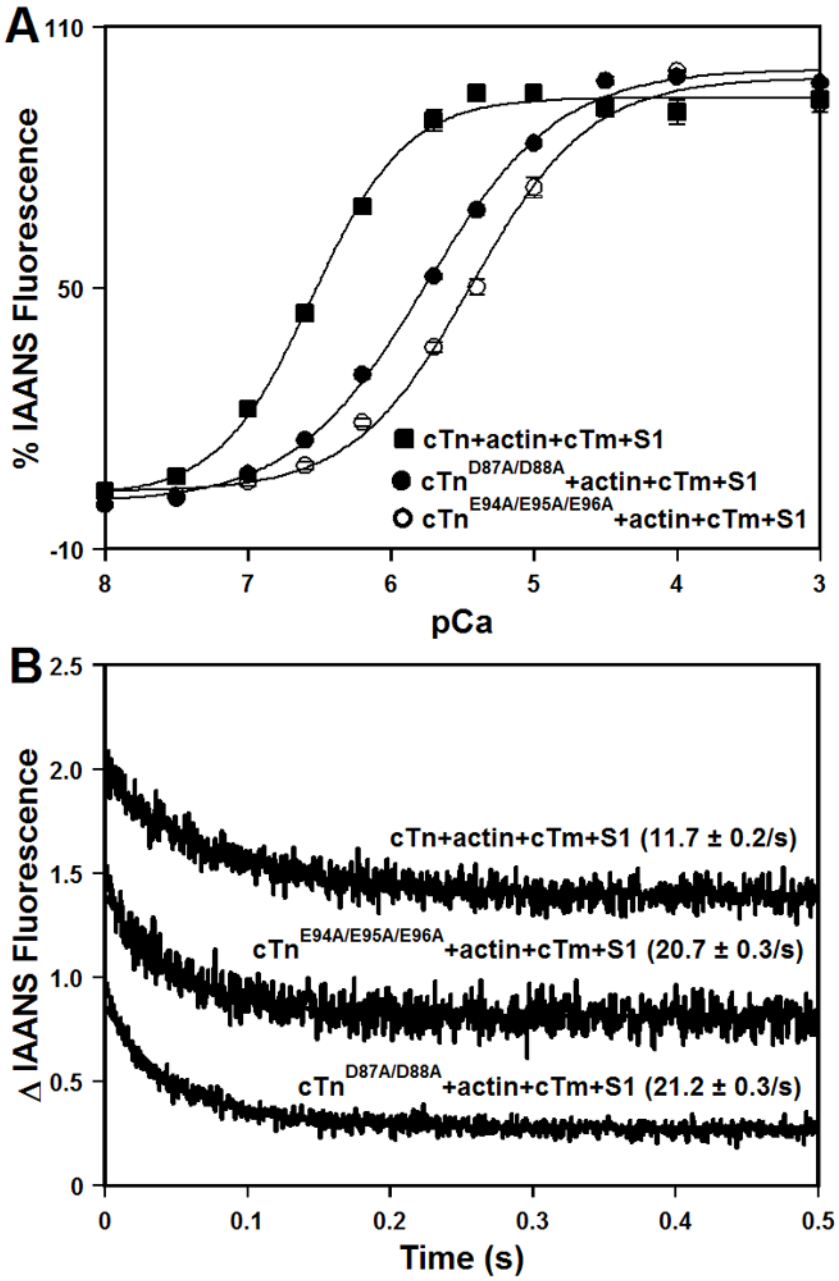

Figure 6. Effect of the central helix mutations on the Ca^{2+} binding properties of reconstituted thin filaments in the presence of myosin S1

Panel A shows increases in IAANS fluorescence, which occur as Ca^{2+} binds to the cTn (■), $cTn^{D87A/D88A}$ (●), or $cTn^{E94A/E95A/E96A}$ (○) complexes reconstituted into thin filaments in the presence of myosin S1 at 15°C. The cTnC proteins (with C35S/T53C/C84S substitution) were labeled with IAANS at Cys^{53}. The IAANS fluorescence was excited at 330 nm and monitored at 490 nm. Panel B shows the time course of decreases in IAANS fluorescence as Ca^{2+} was removed by excess EGTA from the cTn, $cTn^{D87A/D88A}$, or $cTn^{E94A/E95A/E96A}$ complexes reconstituted into thin filaments in the presence of myosin S1 at 15°C. The data

traces have been normalized and staggered for clarity. Each trace is an average of at least five traces fit with a single exponential equation. The IAANS fluorescence was excited at 330 nm and monitored through a 515 nm cut-on filter.

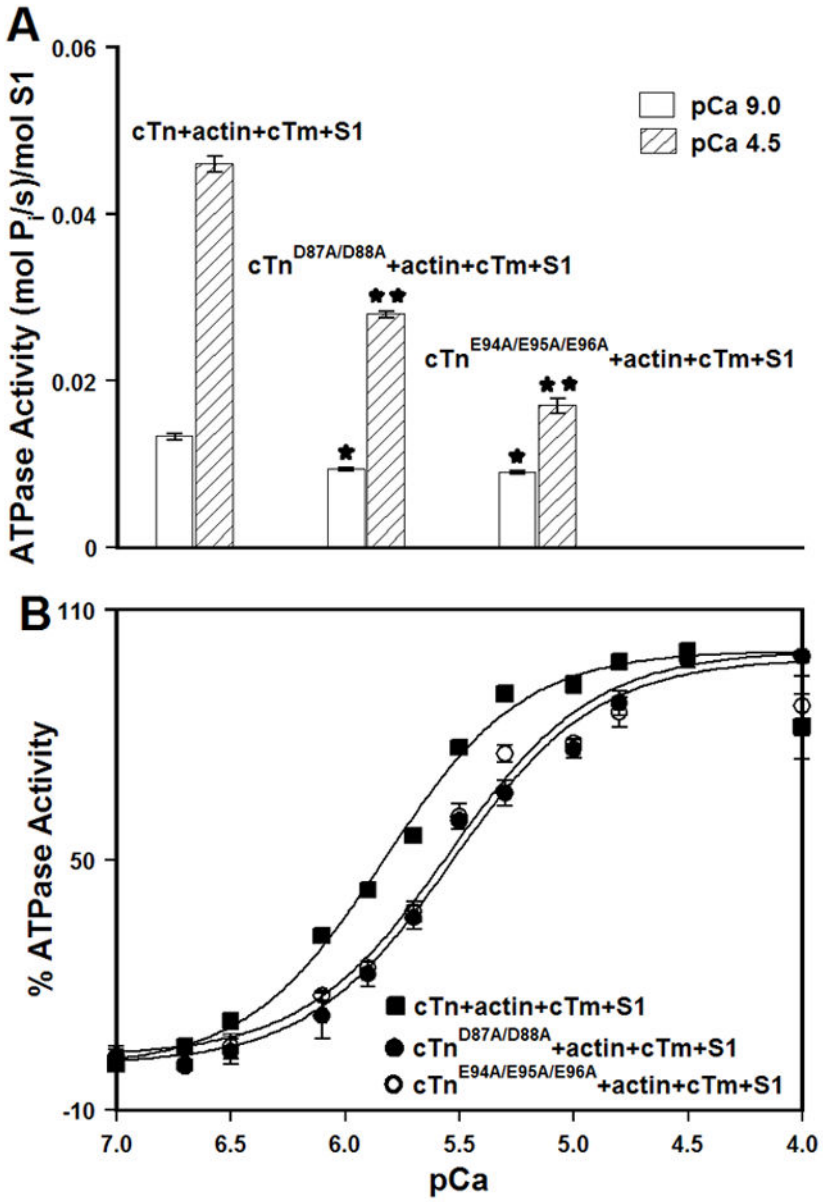

Figure 7. Effect of the central helix mutations on the specific activities and Ca^{2+} sensitivities of actomyosin ATPase

Panel A shows the specific actomyosin ATPase activity of the cTn, $cTn^{D87A/D88A}$, or $cTn^{E94A/E95A/E96A}$ complexes reconstituted into thin filaments (in the presence of myosin S1) at pCa 9.0 (open bars) or pCa 4.5 (bars filled with slanted lines). The cTnC proteins (with C35S/T53C/C84S substitution) were labeled with IAANS at Cys^{53}. Each data point represents a mean ± SE of three separate experiments (each carried out in triplicate). Values marked with * are significantly different from the control values at pCa 9.0 ($p< 0.05$). Values marked with ** are significantly different from the control values at pCa 4.5 ($p<0.05$). Panel B shows the Ca^{2+} dependent activity of actomyosin ATPase for the cTn (■), $cTn^{D87A/D88A}$ (●), or $cTn^{E94A/E95A/E96A}$ (○) complexes reconstituted into thin filaments (in the presence of myosin S1) as a function of pCa. Each data point represents a mean ± SE

of at least three separate experiments (each carried out in triplicate). Data sets were individually normalized for each mutant cTn complex reconstituted into thin filaments (in the presence of myosin S1), and fit with logistic sigmoid.

Table I

Effect of the Central Helix Mutations on the Ca^{2+} Binding Properties of cTnC in Increasingly Complex Biochemical Systems

Biochemical System	Ca^{2+} K_d (μM)	n_H	Ca^{2+} k_{off} (s^{-1})
cTnC	28 ± 2	0.97 ± 0.01	1349 ± 56
$cTnC^{D87A/D88A}$	46 ± 1[a]	0.88 ± 0.01[a]	1360 ± 120
$cTnC^{E94A/E95A/E96A}$	24 ± 1	1.03 ± 0.01[a]	1310 ± 77
cTn	0.83 ± 0.07	0.77 ± 0.02	42.3 ± 0.2
$cTn^{D87A/D88A}$	2.5 ± 0.2[b]	0.89 ± 0.07	82 ± 2[b]
$cTn^{E94A/E95A/E96A}$	1.8 ± 0.1[b]	0.88 ± 0.04	63.7 ± 0.8[b]
cTn+actin+cTm	2.15 ± 0.09	1.62 ± 0.04	93 ± 1
$cTn^{D87A/D88A}$ + actin+cTm	10 ± 1[c]	1.16 ± 0.04[c]	168 ± 2[c]
$cTn^{E94A/E95A/E96A}$ + actin+cTm	12 ± 1[c]	1.47 ± 0.09	164 ± 2[c]
cTn+actin+cTm+S1	0.29 ± 0.02	1.3 ± 0.1	11.7 ± 0.2
$cTn^{D87A/D88A}$ + actin+cTm+S1	1.73 ± 0.05[d]	0.93 ± 0.02	21.2 ± 0.3[d]
$cTn^{E94A/E95A/E96A}$ + actin+cTm+S1	3.7 ± 0.3[d]	1.06 ± 0.07	20.7 ± 0.3[d]

[a] Significantly different from their respective cTnC values ($p<0.05$)

[b] Significantly different from their respective cTn values ($p<0.05$)

[c] Significantly different from their respective cTn+actin+cTm values ($p<0.05$)

[d] Significantly different from their respective cTn+actin+cTm+S1 values ($p<0.05$)

Table II

Effect of the Central Helix Mutations on the Properties of Actomyosin ATPase.

Biochemical System	Activity at pCa 9.0 (mol P_i/s)/mol S1	Activity at pCa 4.0 (mol P_i/s)/mol S1	Ca^{2+} K_d (μM)	n_H
cTn+actin+cTm+S1	0.0133 ± 0.0004	0.046 ± 0.001	1.49 ± 0.03	1.44 ± 0.06
$cTn^{D87A/D88A}$+actin+cTm+S1	0.0094 ± 0.0001[a]	0.0284 ± 0.0004[a]	2.9 ± 0.2[a]	1.4 ± 0.1
$cTn^{E94A/E95A/E96A}$+actin+cTm+S1	0.0090 ± 0.0002[a]	0.0173 ± 0.0004[a]	2.84 ± 0.05[a]	1.4 ± 0.1

[a] Significantly different from their respective control values ($p<0.05$)